ELSEVIER

Journal of Structural Geology 26 (2004) 1401–1418

JOURNAL OF STRUCTURAL GEOLOGY

www.elsevier.com/locate/jsg

Asymmetrical to symmetrical magnetic fabric of dikes: Paleo-flow orientations and Paleo-stresses recorded on feeder-bodies from the Motru Dike Swarm (Romania)

Olivier Féménias[a,b,*], Hervé Diot[b,c], Tudor Berza[d], Antoine Gauffriau[a], Daniel Demaiffe[a]

[a]*Laboratoire de Géochimie Isotopique et Géodynamique Chimique, DSTE, Université Libre de Bruxelles (CP 160/02) 50, av. Roosevelt 1050, Brussels, Belgium*

[b]*Université de La Rochelle, av. Crépeau, 17402 La Rochelle cedex 1, France*

[c]*UMR CNRS 6112, UFR de Sciences et Techniques, BP 92208, 44322 Nantes cedex 3, France*

[d]*Institutul Geologic al Romaniei, Bucharest 78344, Romania*

Received 3 April 2003; received in revised form 1 December 2003; accepted 9 December 2003

Available online 6 February 2004

Abstract

The fabric in a dike is representative of the magmatic flow, considered as Newtonian. The anisotropy of magnetic susceptibility of the rocks gives a good representation of the shape-preferred orientation which, in turn, is a marker of the magmatic flow. Generally, a symmetrical pattern of the fabric across the dike is in agreement with a flow of magma within a channel: the flow direction is then reliable with this imbrication. An asymmetrical fabric is dependent on the flow and displacement of the wall. We present the case of both symmetrical and asymmetrical dike fabrics recording different emplacements. From a Pan-African calc–alkaline dike swarm (of basaltic–andesitic–dacitic–rhyolitic composition) of the Alpine Danubian window from South Carpathians (Romania), two populations of dikes have been described: thick (1–30 m) N–S-trending dikes and thin (<1 m) E–W dikes. The first display asymmetrical fabric and record the regional sinistral movement of the walls. In contrast, the thin dikes are symmetrical and frequently display an arteritic morphology that limits the dike length, with no cartographic extension. We propose to relate the two types of dikes to the same regional stress field in a continuum of emplacement during a regional brittle event.

Keywords: Dikes; Magmatic fabric; Anisotropy of magnetic susceptibility (AMS); Romania

1. Introduction

The four dikes studied in this work come from a large Pan-African calc–alkaline dike swarm (the Motru Dike Swarm: MDS) that occurs in the Alpine Danubian window of the South Carpathian mountains in Romania (Fig. 1). The detailed sampling of these dikes has allowed us to distinguish two populations of dikes, on the basis of their sizes and asymmetrical or symmetrical characteristics. We attempt to use measured magnetic data to infer the differences of mode of emplacement between thick (several meters up to 1.5 m) and thin dikes.

* Corresponding author. Correspondence address: Laboratoire de Géochimie Isotopique et Géodynamique Chimique, DSTE, Université Libre de Bruxelles (CP 160/02) 50, av. Roosevelt 1050, Brussels, Belgium. Tel.: +32-2-650-2254; fax: +32-2-650-2226.

E-mail address: ofemenia@ulb.ac.be (O. Féménias).

0191-8141/$ - see front matter © 2004 Elsevier Ltd. All rights reserved.
doi:10.1016/j.jsg.2003.12.003

2. Geological setting

The South Carpathian crystalline units were thrust upon the Moesian cratonic platform in Upper Cretaceous to Tertiary times and have been partly covered by Cenozoic sediments in erosion discordance. The various Eoalpine (Cretaceous) Danubian nappes have been subdivided in Upper and Lower Danubian (Berza et al., 1983, 1994) on the basis of their Mesozoic cover (Stănoiu, 1973; Kräutner et al., 1981). The Lower Danubian nappes of Lainici and Schela-Petreanu (Kräutner et al., 1981, 1988; Berza et al., 1994) contain the same basement lithologies (Berza and Seghedi, 1983). They consist of two Pan-African terranes (Liégeois et al., 1997): the Lainici-Păiuş (Manolescu, 1937) migmatitic unit and the Dragsan (Pavelescu, 1953) amphibolitic unit intruded by several post-metamorphic granitoids and

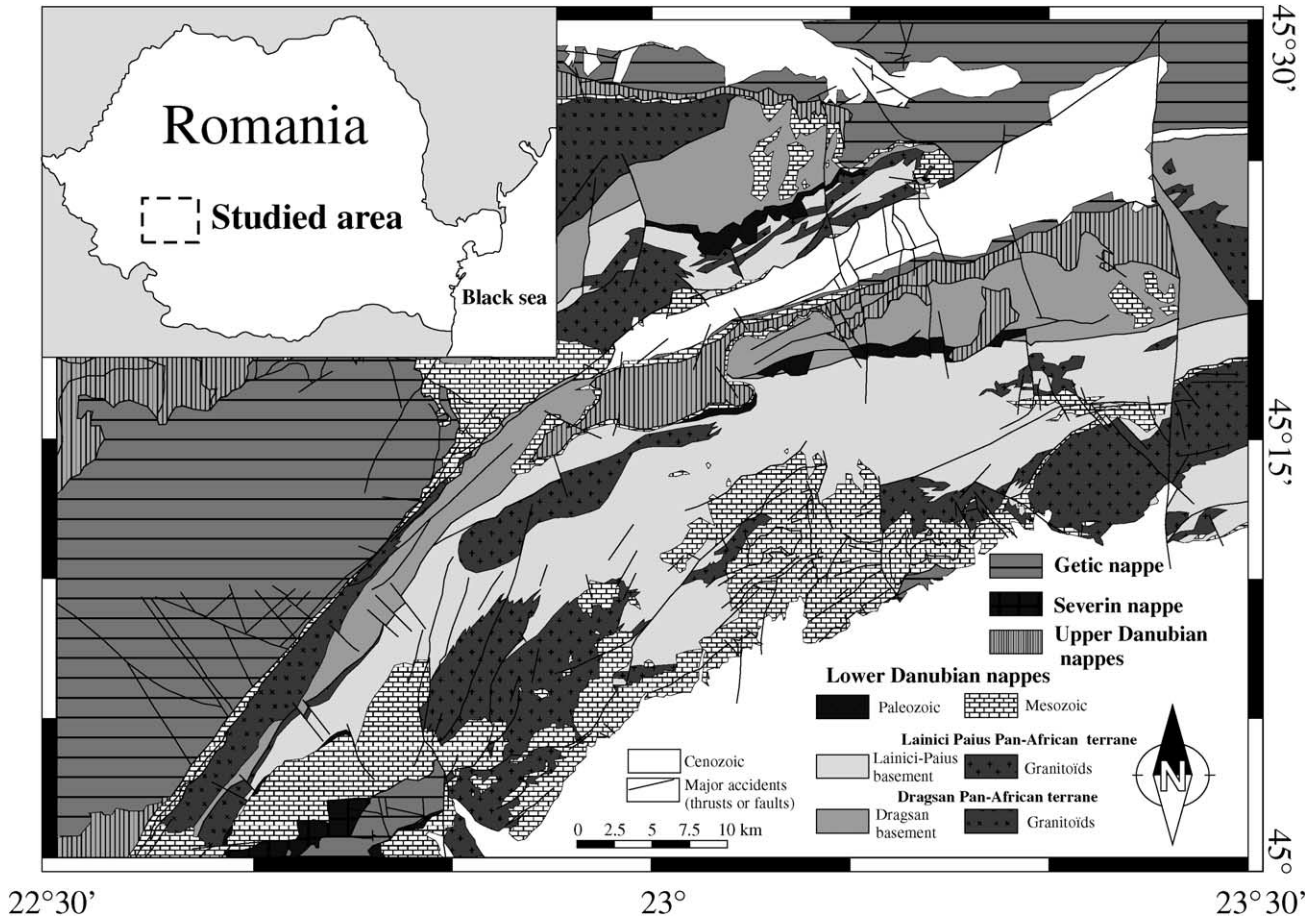

Fig. 1. Map of the pre-Alpine units of the South Carpathian Mountains, from the IGR 1/50,000 map, modified after Berza et al. (1994).

capped by Upper Ordovician–Devonian sediments. The tectonic contact between these two units has been attributed to the Variscan orogen (Berza and Iancu, 1994). The Lainici-Păiuş unit is essentially composed of quartzite, biotite gneiss, marble, graphitic gneiss and leucrogranite bodies, dikes and sills that form an important migmatitic complex. This unit is characteristically affected by a low-pressure/high-temperature amphibolite metamorphism (Savu, 1970; Berza, 1978). It is intruded by large, elongated, calc–alkaline to shoshonitic plutons (i.e. the Tismana pluton; Duchesne et al., 1998). The last (pre-Silurian) magmatic event corresponds to the intrusion of the MDS (Berza and Seghedi, 1975) that, contrary to the leucogranite dikes, crosscut the plutons. The MDS has been systematically investigated in the Lainici-Păiuş geological unit and the area south of the Frumosu intrusion. These areas have been chosen for AMS investigations due to the weakness of Alpine deformations (lack of a penetrative cleavage) and only marked by the development of chlorite along decameter- to meter-spaced joints. Country rocks are dominantly leucogranitoid bodies and quartzites showing Pan-African ductile deformation in a deep structural level.

Detailed field investigations have allowed us to distinguish the two populations of dikes that both crosscut the country rocks without chronological relations between them (no observation of continuity between the two). The first population of dikes is characterized by thin section (<1 m) and a N80° mean direction (Fig. 2A); the second population displays thicker section (several meters up to 1 m) and a N–S orientation (Fig. 2B). The two large dikes investigated (TJ30 and TJ34) show sinistral shearing along their walls, as suggested by a penetrative cleavage of their chilled margins (and enhanced erosion). This shear is not recorded in the country rocks, implying that it was recorded at the end of the dike emplacement.

The MDS is essentially composed of andesitic to dacitic dikes; andesitic basalt and rhyolite are less common. The textures are aphyric to microgranular. Porphyritic andesites contain euhedral tschermakite ± clinopyroxene and plagioclase, while porphyritic dacites have euhedral plagioclase, magnesiohornblende and/or partly resorbed quartz. Plagioclase is often deeply retrogressed to epidote ± calcite ± white mica and appears commonly as ghost. In andesitic rocks, the groundmass consists of tiny quartz, plagioclase, ferromagnesian phases (amphibole and rarely clinopyroxene), oxides and devitrified glass. Mn-rich ilmenite is the main opaque phase; it occurs either as euhedral to subhedral

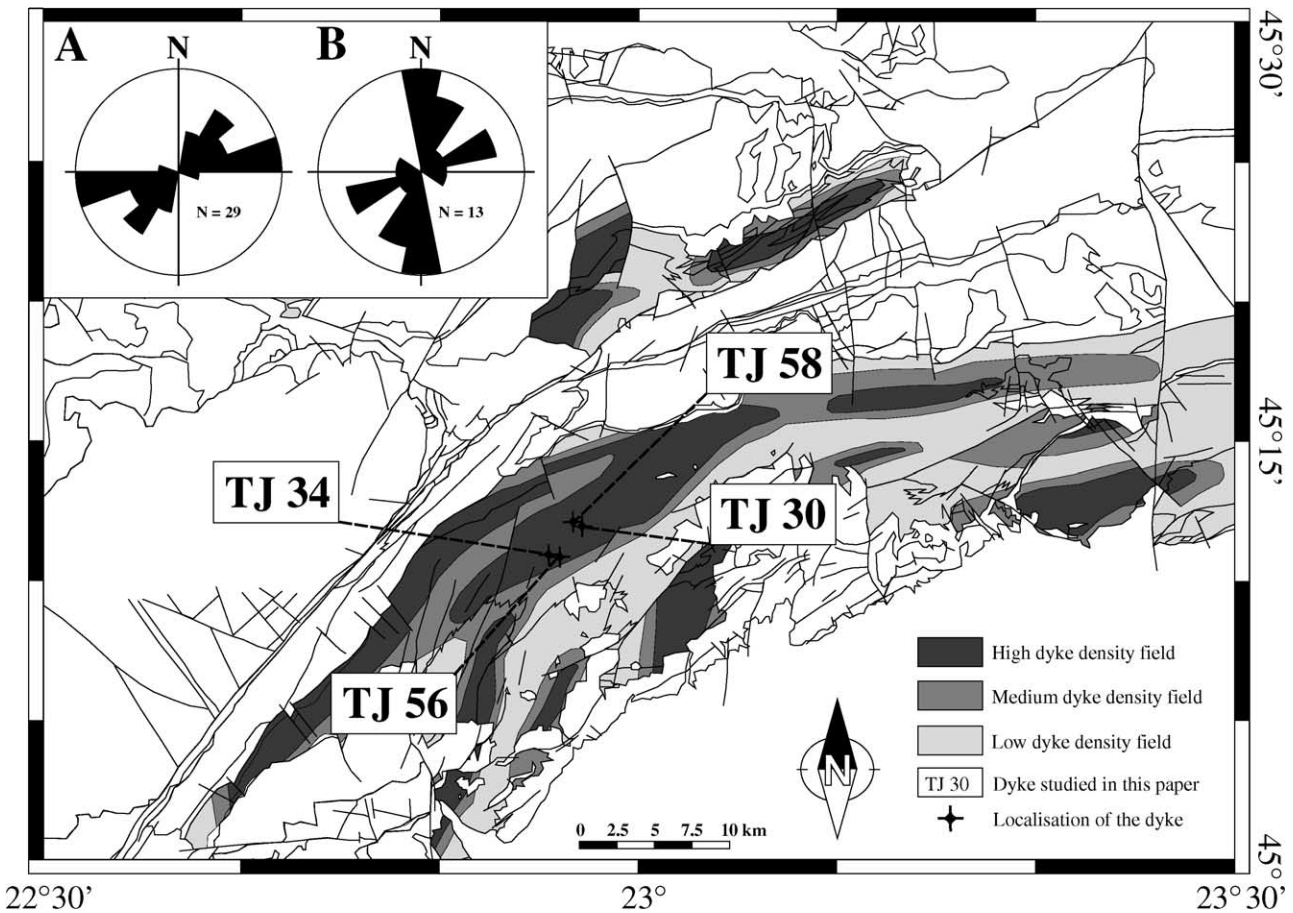

Fig. 2. Map of the relative distribution of the dikes of the Motru Dike Swarm into the Lainici-Păiuş unit and position of the studied dikes. From the 1/50,000 IGR map. (A) Rose distribution diagram of the thin dikes. (B) The same for the wide dikes.

crystals and glomeromorphic (mean grain size, 100–400 μm) or as single (a few tens to 100 μm) anhedral to skeletal grains. Deuteritization and propylitization occur during and just after the dike emplacement and induce a low temperature–low pressure secondary paragenesis. Locally, Ti-bearing silicate phases have been pseudomorphosed to a leucoxene assemblage; chlorite, calcite, talc, epidote and pyrrhotite-pyrite (altered to goethite and hematite) developed locally as millimeter-size euhedral grains.

TJ30 is a porphyritic dacite with plagioclase phenocrysts and scarce quartz. TJ34 is a fine-grained biotite- and amphibole-bearing andesite with scarce sulfides and oxides. TJ56 and TJ58 are, respectively, an aphyric andesite and a (micro)-amphibole-rich andesite. TJ30 and TJ56 are mineralogically homogeneous along their widths, whereas TJ58 and TJ34 show strong heterogeneities in oxide and ferromagnesian mineral distributions between core and rim (TJ58) and inside the body itself (TJ34). The thin (decimeter-sized) dikes TJ56 and TJ58 have chilled margins that consist of microphenocrysts of plagioclase and clinopyroxene in a secondary (= deuteritic) groundmass. The thick (several meters) TJ30 and TJ34 dikes also present aphyric chilled margins where they have a localized late-emplacement cleavage.

3. Theoretical considerations

3.1. Kinematics of lava flow

The kinematics of lava emplacement recorded in the solidified rock as foliation and lineation, gives information on the end of fabric history (Fernandez and Laporte, 1991) and flow direction in dikes (Archanjo et al., 2000). Dike emplacement in a given tectonic setting has to record differential stress involving the combined effect of both external and internal stress fields (Correa-Gomes et al., 2001). Moreover, the arrangement of fabrics gives information on the sense of shear and the shape of strain ellipsoid (ϵ_1, ϵ_2 and ϵ_3 axes) can also, in some cases, be connected to the fabric. Finite deformation state and shape of magmatic fabric are globally related to (1) the viscosity contrast between stress markers and matrix, (2) the percentage of crystal and their nature, (3) the mechanical dragging of phenocrysts during flow, (4) the kinematics of flow, (5) the nature of successive intrusions, and (6) the deformation history (Gay, 1968; Fernandez and Laporte, 1991; Ildefonse et al., 1992a,b; Wada, 1992; Correa-Gomes et al., 2001). The different recorded types observed in the MDS are referred to the same geological setting characterized by a

regional differential stress. Contemporaneous dikes display variations in size and fabric involving different families related to particular developments and dikes emplacement. These dike families are linked to different rates of lava displacement and stages of dike emplacement, lead to regional structuration or lead the fracture system to the main magmatic flow (Baer, 1995).

3.2. AMS investigation and relation between fabric and flow

Fine-grained crystalline and/or aphyric cryptocrystalline sub-volcanic textures do not easily allow the estimation of fabrics or sub-fabrics defined by ordered orientation and/or gathering of crystals and by many other structural orientations from macroscopic to microscopic size. Unfortunately, macroscopic flow indicators are scarce, but field or petrographic studies of shape preferred orientations (SPO) of crystal can be completed using magnetic subfabric surveys deduced from measurements of the anisotropy of magnetic susceptibility (AMS). This method is indeed sensitive enough to determine the subtle fabrics in lava flows even when they are poorly (only a few percent) anisotropic (Knight and Walker, 1988; Cañón-Tapia et al., 1996). Magnetic fabric, i.e. SPO of magnetic mineralogy (except in the case of rare, possibly magnetite, interactions when crystals of a sufficient amount in lava are organized along oblique clusters; Grégoire et al., 1998; Cañón-Tapia, 2001), has also been investigated in numerous cases and appears to be a good subfabric of the real magmatic fabric (bulk shape preferred orientation of crystals in a magmatic medium). Nevertheless, the assumption that the principal magnetic vector, K_1, represents the flow direction everywhere through a dike is not always verified (Rochette et al., 1999; Callot et al., 2001; Geoffroy et al., 2002) but the flow could be approached by the local or mean orientation of imbricate foliations along the dike's walls. Such structural figures was effectively postulated by Knight and Walker (1988) and extensively used by a wide variety of workers (e.g. Nicolas, 1992; Tauxe et al., 1998; Herrero-Bervera et al., 2001) to mark a double imbrication against the two dike margins, and to infer the azimuth of flow. These models of flow vector calculation are, however, based on a theoretical symmetrical fabric of the dike that has not been debated enough in the past. Recent conceptual models (Correa-Gomes et al., 2001) integrate the idea of an anisotropic regional strain field during dike emplacement and the necessary existence of both symmetrical and asymmetrical dike fabrics in which magma flow direction is represented by a global vector, defined by the summation of the magma flow itself and the tectonic movements along the dike walls.

In the case of a symmetrical opening of a dike without transcurrent component, we propose to describe the flow through a 'Newtonian' dike model (Fig. 3a). This is based on several arguments: experimental flowing evidence (Merle, 1998), theoretical evidence (Komar, 1972a,b, 1976), observation of strained vesicles (Coward, 1980; Rust and Manga, 2002), evolution of a magmatic fabric during a simple shear (Ildefonse and Fernandez, 1988; Ildefonse et al., 1992a,b; Arbaret et al., 1996, 2000, 2001; Marques and Coelho, 2003) or a combination of simple and pure shear (Ježek et al., 1996). We consider that the flow pattern induces the coexistence of two strain regimes, evolving from simple shear, near the dike's wall to a mainly pure shear in the core of the dike (Fig. 3a). As a consequence, the symmetrical flow pattern and the inversion of the passive marker's finite strain ellipsoid axis (vesicles) are also recorded by an active marker's fabric such as: (1) an oblique to sub-parallel foliation (with an angle, α, between the dike's wall and the foliation dependent on the shear intensity) near the rim and a perpendicular foliation in the core of the body; (2) an imbrication of the foliations from each side of the dike (depending on the α-angle); (3) a lineation parallel to the flow vector near the wall and perpendicular to this vector in the core, with an intermediate inversion of the K_1–K_2 axis (Fig. 3a); (4) different domains of strain: a prolate ellipsoid is theoretically representative of the rim and an oblate one of the core. The stabilization of the fabric is, however, well-defined; it is sub-parallel to the wall plane (low values of α-angle) as long as a simple shear is assumed. The departure of this position increases towards the core where pure shear is dominant and responsible for the inversion of the fabric axis (both active and passive maker's fabric have identical orientation).

Nevertheless, even if a stabilization of the fabric can occur near the wall, this ideal pattern is certainly not realistic. Indeed, in a natural magmatic body, the rheology cannot be considered as constant, across and along the dike. It varies strongly with mechanical, thermodynamical and chemical conditions. These rheological variations (from Newtonian to Binghamian) occur classically during magma's cooling by growth of crystals along the walls and mineral flowage differentiation towards the core (Bagnold, 1954; Komar, 1972a,b, 1976). So, the fabric acquisition can be discussed as a time-dependant superposed symmetrical non-Newtonian (Bingham) flow pattern (Fig. 3b). The successive fabrics are thus acquired during the different stages of crystallization and emplacement. Each fabric overprints older time-related foliations during the progressive cooling. This process can also be responsible for the stabilization of the position of the strain ellipsoid axes. The foliation and lineation (without fabric or magnetic axes inversion) should stay parallel to the wall-surface at a given time-cooling distance from the wall, including the internal zones of the body (Fig. 3b) when $t \rightarrow \infty$. This situation can evolve by a change of the flow direction into the dike: from a vertical ascent of the magma rising from a feeding-zone, a horizontal flow occurs as a response to the closing (freezing) of the upper part of the dike (Fig. 3c). This situation induces a magmatic fabric that can be geometrically comparable with the first case (Fig. 3a), but this fabric is here associated with a horizontal simple shear in the core of the dike.

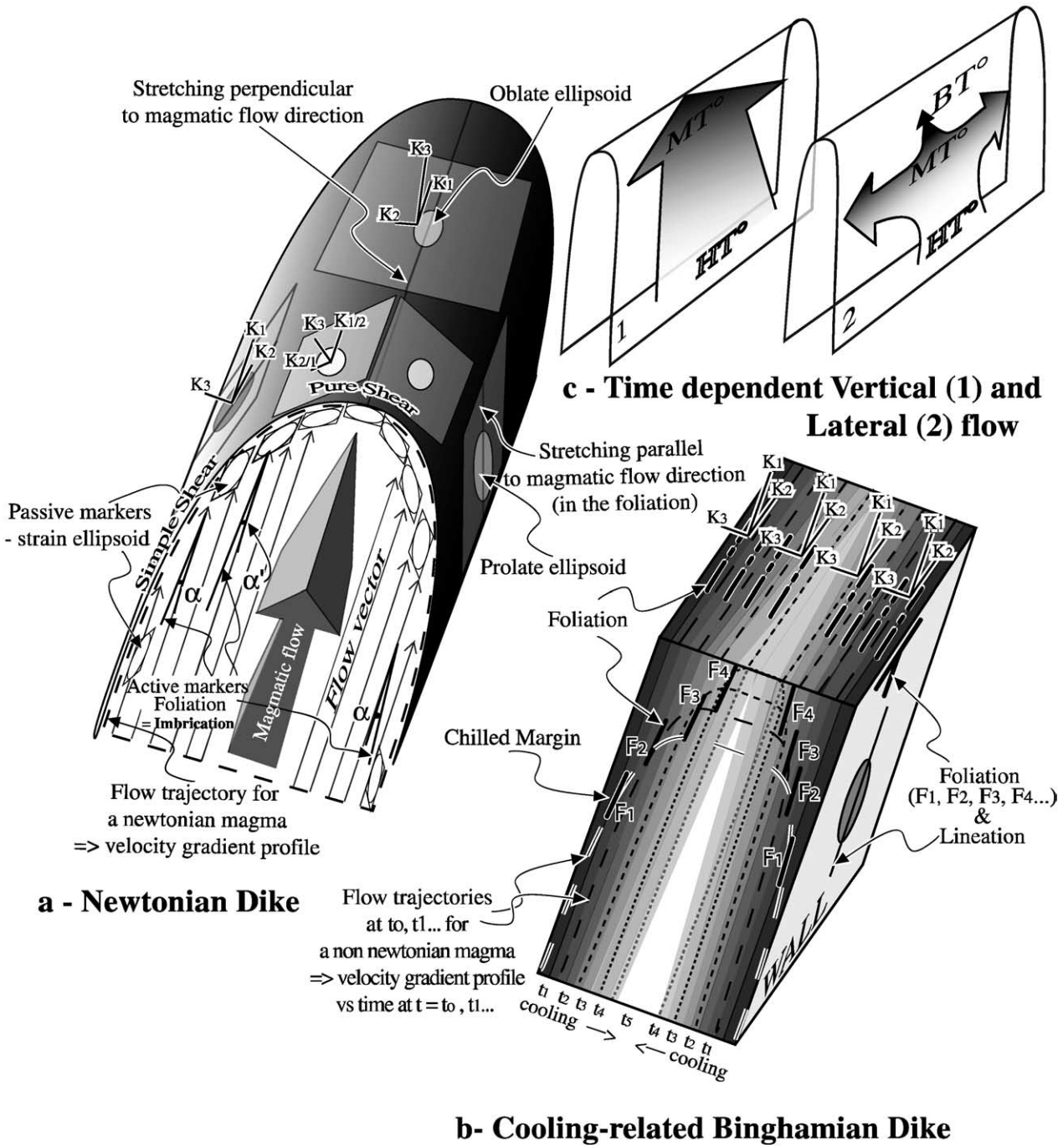

Fig. 3. Schematic sketches illustrating different models of relation between flow, viscosity and internal fabric of dike. (a) Representation of a 'Newtonian dike' including structures acquired, respectively, by passive and active markers from the wall to the center of the dike. (b) Representation of a 'cooling-related Binghamian dike'; t_1 to t_5 represent time steps of the cooling history. (c) Evolution of the flow in time for a cooling-related Bingham type of dike. See text for explanation.

Thus, these two conceptual processes of emplacement ('Newtonian' and 'cooling-related Binghamian' dikes) involve two contrastive fabrics in a dike (Fig. 3a and b). Up to now, a few geological criteria only are available to distinguish these two fabrics: width and lateral extension of the dike, relationship between dikes of different orientations, relationship with the country rocks, crystal matrix ratio in each zone of the dike, macroscopic fabric, vesicle fabric, etc. AMS data and especially AMS parameters P' and T can also give information in order to distinguish between these different types of emplacement. From this association with the geometric characteristics of each type, a relative higher value of P' near the wall of the dike would be representative of a Newtonian type (Fig. 3a) where the core is mainly a domain of translation of the magma. On the contrary,

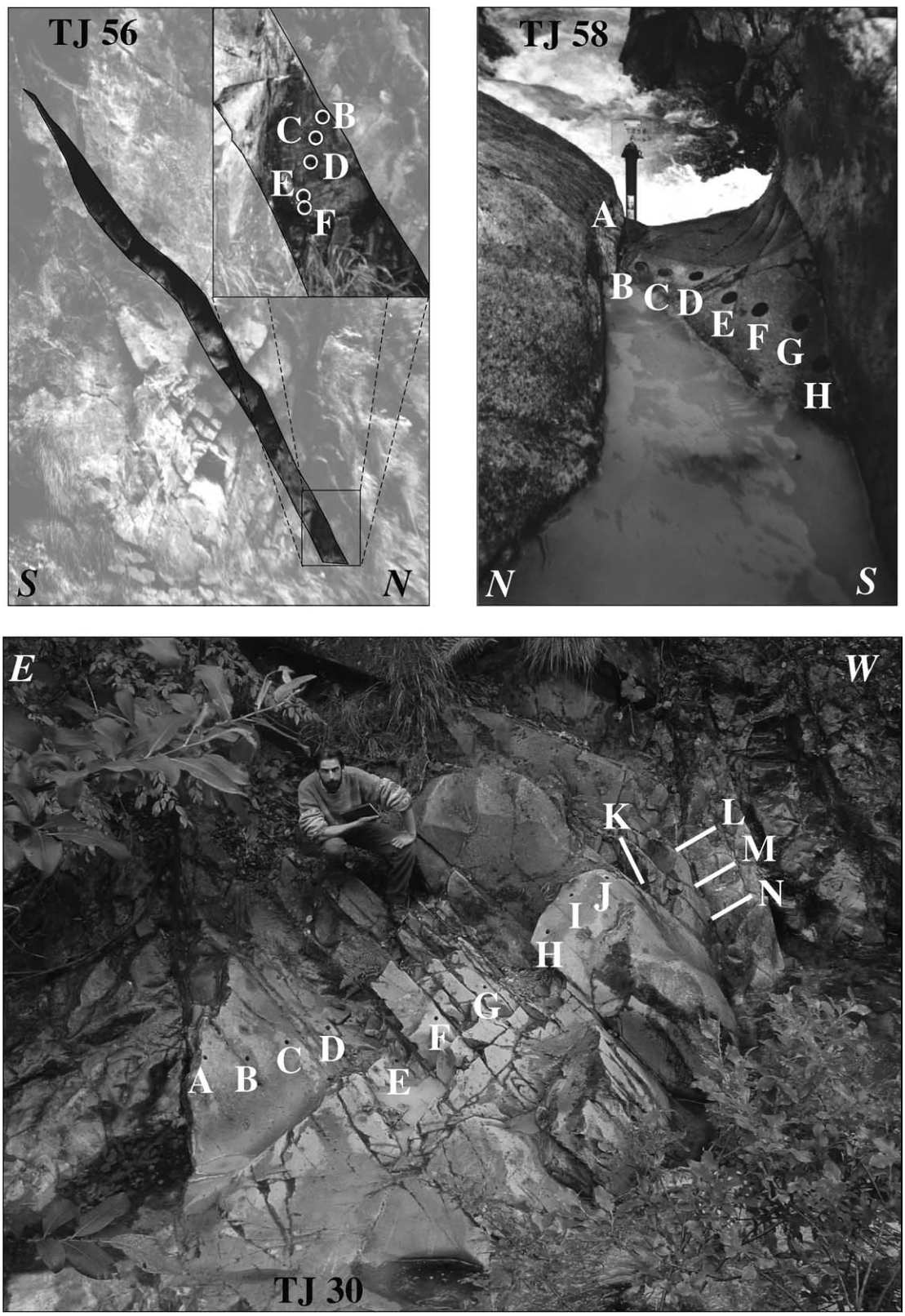

Fig. 4. Photographs of the two arteritic dikes presented in this study (TJ56 and TJ58) and a wider one (TJ30). Letters refer to core-drilled samples.

high values of P' would be found in the core of cooling-related Binghamian type dikes.

Following this idea we have interpreted our AMS results to characterize the fabric and development of dikes in term of magmatic flow. Moreover, by contrast with Herrero-Bervera et al. (2001) and Geoffroy et al. (2002), we do not suppose a symmetrical arrangement of AMS axes around the principal plane of the dike in order to look at a possible transcurrent displacement of the walls during emplacement (Correa-Gomes et al., 2001). For this objective, a systematical sampling of the complete sections across the studied dikes has been realized.

4. Sampling and measurement procedures

Two localities, in the same area, have been chosen because they both show the two types of dikes (Fig. 2). For the four dikes sampled for AMS measurements, the contact with the wall rocks are well exposed. Sampling intervals across the dike's width have been adapted according to their thickness. The 23-m-thick TJ34 dike has been sampled at 24 stations, the 2.5-m-thick TJ30 dike at 14 stations and the thin dikes, TJ58 (70 cm thick) and TJ56 (30 cm thick), at 8 and 5 stations, respectively (Fig. 4). Sampling has been performed with a portable drilling machine and, at each station, an oriented sample (25-mm-diameter) has been cored.

Each drill core has been cut into two or three 22-mm-high cylinders. The AMS measurements were performed on the upper part of each drill core, using a Kappabridge KLY-3S susceptometer (AGICO Ltd) working in a weak alternative field whose resolution is better than 10^{-8} SI. For each cylinder, the measurement provides the magnitudes of the three principal, mutually orthogonal axes of the AMS ellipsoid ($K_1 \geq K_2 \geq K_3$), as well as their azimuth and inclination with respect to the specimen frame and, after averaging for each of the stations, with respect to the geographical frame.

5. AMS results

5.1. Magnetic susceptibility and anisotropy

The bulk magnetic susceptibility magnitude K_m is given by the arithmetic mean of the K_1, K_2 and K_3 lengths: $K_m = (K_1 + K_2 + K_3)/3$. For the measured samples, K_m values range from 175 to 1330 μSI (Table 1) with a mean value of 465 μSI and a bimodal frequency distribution (Fig. 5a). These magnitudes show that paramagnetic phases could be the principal contributors to susceptibility variations in agreement with the high amphibole and biotite modal content in many samples. Nevertheless the high values of K_m (>500 μSI) of some samples are presumably due to the contribution of magnetite and also of the propylitic sulfide

Table 1
AMS data for the four dikes presented. K_m: magnitude of the bulk magnetic susceptibility; P' and T: anisotropy degree and shape parameters of Jelinek (1981) (see text for definition); K_1 and K_3: long and short principal axes of the AMS ellipsoid; az. and inc.: azimuth and inclination, respectively, of the axes

	K_m (μSI)	P'	T	K_1 az.	K_1 inc.	K_3 az.	K_3 inc.
TJ34							
a	317	1.03	0.55	261	56	119	28
b	380	1.06	0.29	262	64	101	24
c	335	1.03	0.37	236	60	115	17
d	392	1.04	0.11	260	67	119	18
e	421	1.04	0.32	259	74	108	14
f	365	1.05	0.39	224	64	118	7
g	440	1.04	0.42	268	67	124	19
h	398	1.06	0.38	250	56	119	24
i	429	1.11	−0.01	247	48	96	38
j	604	1.09	−0.13	273	59	109	30
k	1058	1.21	−0.11	285	63	103	27
l	446	1.16	0.08	253	59	109	26
m	1192	1.27	−0.22	295	56	94	32
n	1058	1.36	−0.21	279	47	118	41
o	546	1.03	0.27	235	60	122	13
p	392	1.02	0.18	247	54	117	25
q	360	1.02	0.63	273	66	118	22
r	376	1.04	0.32	268	50	126	34
s	315	1.04	0.56	235	37	126	24
t	361	1.09	0.62	230	35	118	28
u	390	1.05	0.38	246	58	117	22
v	524	1.03	0.52	221	65	113	25
w	1085	1.34	0.28	248	46	118	32
x	330	1.03	0.56	227	33	131	9
TJ56							
b	524	1.06	0.38	270	54	130	36
c	507	1.06	0.36	260	45	132	45
d	602	1.10	0.13	266	48	124	42
e	454	1.07	0.39	266	46	128	44
f	526	1.05	0.48	275	47	135	43
TJ30							
a	197	1.07	0.72	234	45	139	5
b	175	1.06	0.86	256	68	138	10
c	188	1.07	0.53	229	64	133	3
d	214	1.10	0.42	266	76	136	9
e	205	1.10	0.50	203	66	313	9
f	202	1.05	0.55	213	31	123	1
g	218	1.08	0.40	220	67	310	0
h	193	1.06	0.35	229	64	139	26
i	204	1.08	0.44	254	69	137	10
j	206	1.08	0.51	267	72	137	12
k	214	1.09	0.29	265	71	137	12
l	252	1.18	0.31	265	67	142	13
m	257	1.31	0.23	243	56	137	10
n	465	2.25	0.07	215	50	117	7
TJ58							
a	445	1.04	0.68	285	59	151	23
b	455	1.03	0.45	277	49	159	22
c	707	1.22	−0.07	294	60	174	17
d	1330	1.34	−0.06	286	58	153	23
e	950	1.27	0.21	294	72	154	14
f	611	1.12	0.14	266	40	157	22
g	435	1.03	0.42	259	32	153	24
h	455	1.04	0.47	280	55	164	17

K_1 and K_3 values are given without rotation of the wall in a vertical plane.

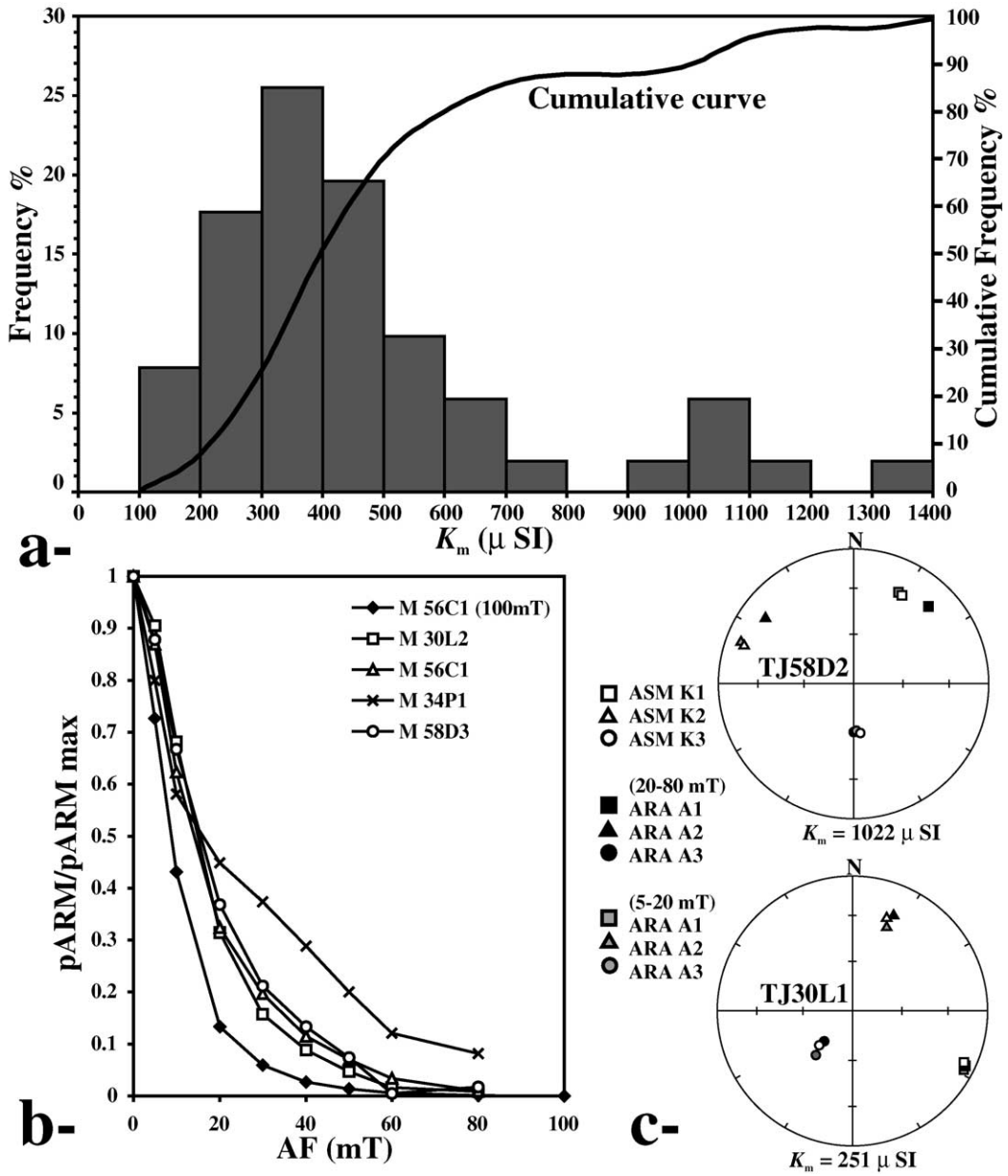

Fig. 5. (a) Histogram and cumulative curve of the susceptibilities measured in the Motru Dike Swarm (see text for explanation). (b) Normalized coercivity spectra of four specimens representative of AMS sites. The spectra show (except for M34P1) a pAARM peak for AF values <20 mT, followed to the right part of the spectra by a smooth decrease down to the background remanent magnetization (attained after 60 mT). The transition for each sample is representative of the magnetic mineralogy (see text for explanation). (c) Schmidt stereoplots (lower hemisphere) of AMS, $pAARM_{5-20}$ and $pAARM_{20-80}$ directional data for two samples (among pAARM measurements). Square, triangle and circle are, respectively, long, intermediate and short axes of the ellipsoid for individual specimens; in white, gray and black: respectively, AMS, $pAARM_{5-20}$ and $pAARM_{5-80}$ data. The coaxiality is well established for the pole of the plane (circle) for both and a good correlation exists for the other axis (see text for explanation).

and associated hematite. By contrast, samples from TJ30, which have low magnitude susceptibility values (<465 μSI) have low amphibole content and no significant opaque content. As the magnetic susceptibility of ferromagnetic minerals is several orders of magnitude larger than that of the most common paramagnetic minerals (Rochette et al., 1992), the magnetic susceptibility of high-K_m samples is due to the ferromagnetic material. This agrees with the cumulative frequency distribution of K_m (Fig. 5a) that suggests that the magnetic mineralogy is dominated by a single magnetic domain because the susceptibility of biotite and amphibole are closed in intensity (Borradaile and Henry, 1997); the very high K_m values (>1000 μSI) are indeed indicative of a ferromagnetic behavior (Rochette, 1987).

The variations of K_m from rim to core in several dikes (Figs. 6A–D and 7) can be due to two parameters: (1) the variations of the modal proportions of amphibole phenocrysts: these variations can themselves result from mechanical segregation by 'Bagnold's effect' of phenocrysts

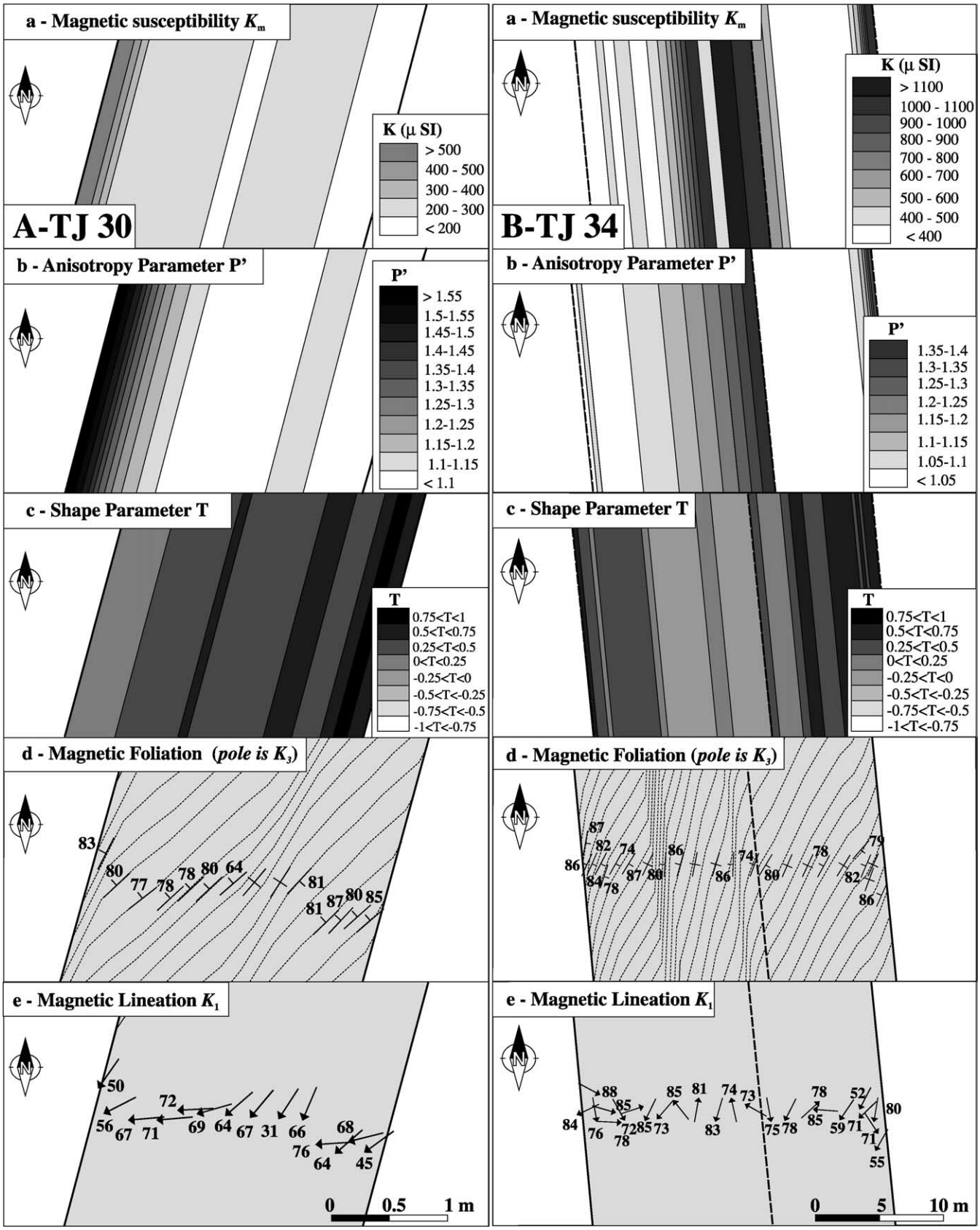

Fig. 6. Magnetic susceptibility (a), anisotropic parameters P' (b) and T (c), magnetic foliation (d) and lineation (e) views in maps for the dikes TJ30 (A), TJ34 (B), TJ56 (C), and TJ58 (D) with a vertical representation of the walls.

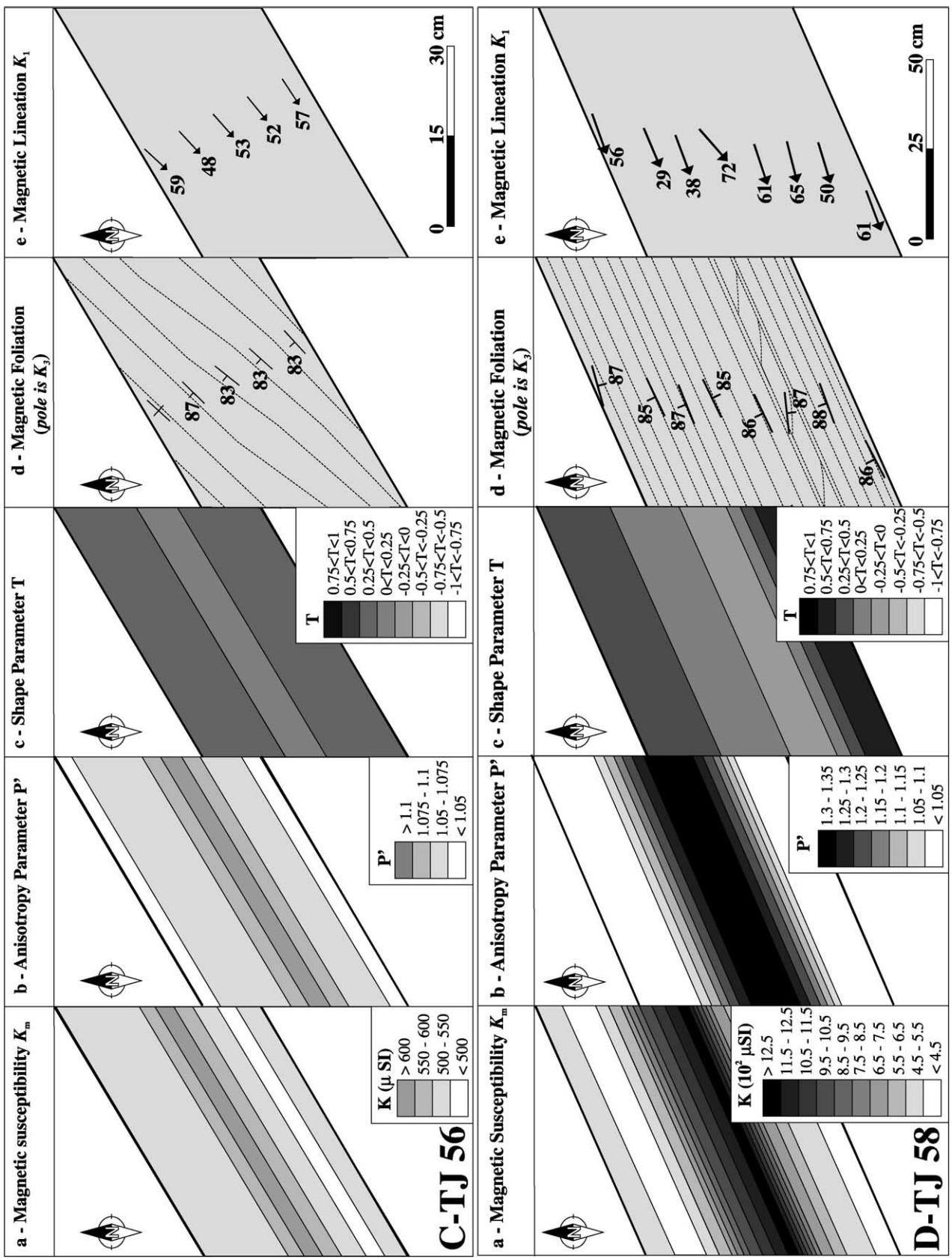

Fig. 6. (*continued*)

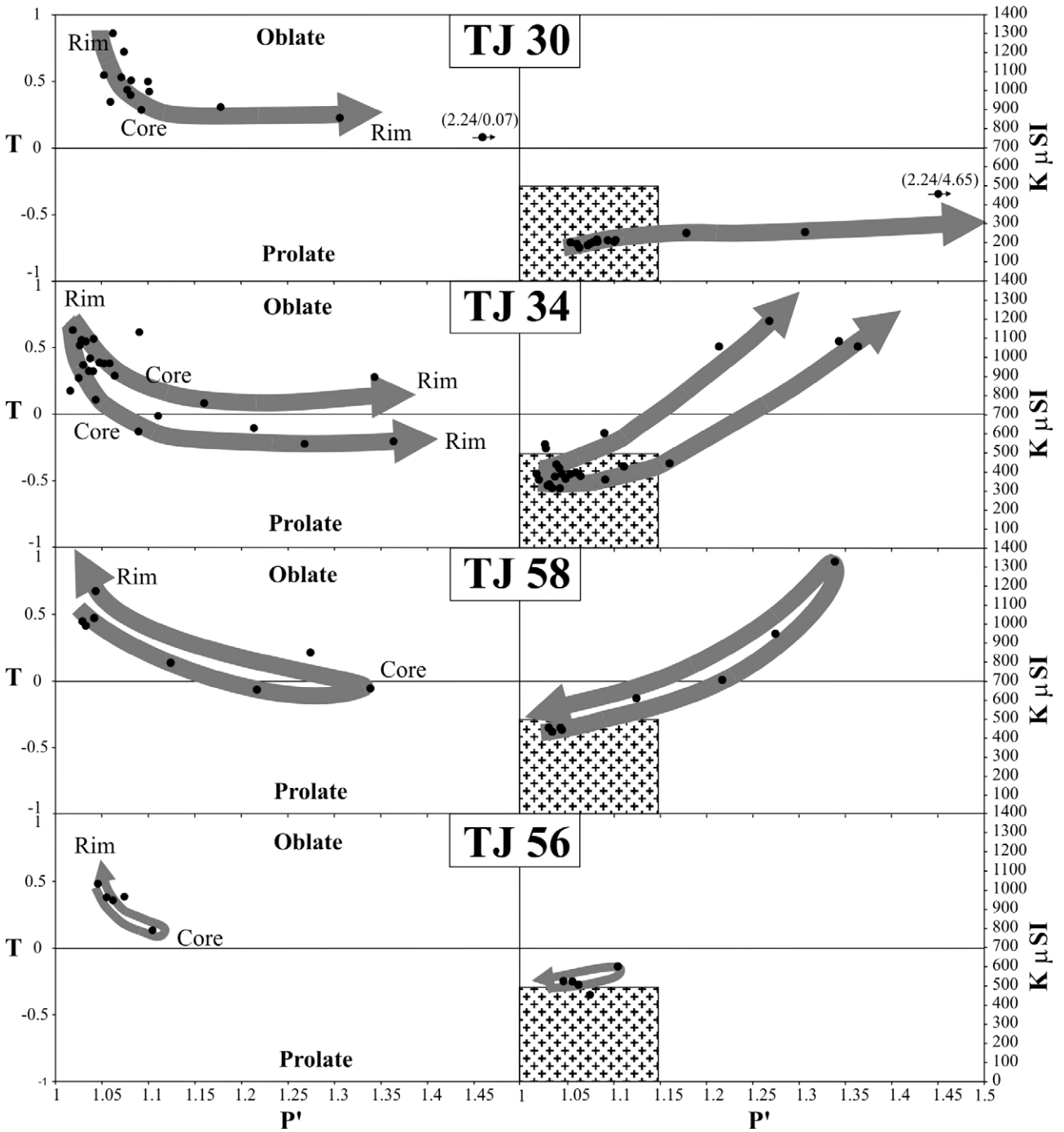

Fig. 7. T (to the left) and K (to the right) versus P' and trend (gray arrow) from rim to core for each studied dike (see text for explanation).

representing pre-injection mineral phases (Bagnold, 1954; Komar, 1972a,b, 1976; Barrière, 1976) during dike emplacement and successive pulse of magma, and (2) late-emplacement fluid percolation along canalized conduits. This second mechanism could explain the observed correlation between the K_m variations and the abundances of propylitic iron sulfide and associated hematite. The pyrrhotite-pyrite development and localization in the dike is presumably related to the iron remobilization during retrogression of the ferromagnesian silicate phases; this could enhance the magnetic signal due to the primary amphiboles and magnetite. Thus, the value of K_m clearly appears to be a good indicator for mapping the petrological and structural boundaries in complex dikes resulting from several injections (Fig. 6Ba for TJ34) and/or secondary retrogression.

As the magnetic mineralogy of the samples is very complex, with various para- and ferromagnetic minerals, it

was investigated through coercivity spectra on individual rock cylinders for eight representative samples. These spectra (made with a LDA3-AMU1 apparatus and a JR5A spinner magnetometer of Agico Ltd) are acquired after AF demagnetization at 100 mT, at intervals of 10 mT from 0–10 up to 100 mT with a DC field of 0.05 mT. The curves (Fig. 5b), exhibit high values at low AF values followed by a smooth decrease down to the background remanent magnetization. This weak residual remanence is attained after 60 mT for most specimens but remains at a high value for sample 34P, which particularly reveals the presence of strongly coercive secondary hematite. These coercivity spectra, from low to high coercivity, reveal a repetitive heterogeneity of the magnetic mineralogy, i.e. the co-existence of different magnetic mineralogy: high and medium coercive fractions can be linked with the presence of magnetite of various grain sizes (Jackson et al., 1988) but observed sulphides can contribute for a part of the spectra in addition to the paramagnetic silicates phases.

Anisotropy of magnetic susceptibility in rocks dominated by amphibole and magnetite in various amounts and sizes (and locally by iron sulfide and/or hematite) results mainly from the shape-preferred orientation of these grains, even if possible interactions between magnetite organized in clusters of grains describing a distribution anisotropy only play a minor role (Hargraves et al., 1991). In the studied dikes, due to the relatively lower susceptibility and the probable magmatic origin, the distribution of grains of magnetite in space is more distant than their diameter (Grégoire et al., 1998). Thus, magnetic interaction is highly unlikely, and the origin of magnetic anisotropy appears to be mainly controlled by the individual anisotropy of each grain. The iron sulfide occurs as isotropic euhedral shape, with hematite as anhedral with interstitial habitus, underlining the diamagnetic and paramagnetic mineral sub-fabric. In order to link AMS and petrofabric i.e. to validate the use of AMS method for our samples, as AMS represents the sum of magnetic contributions from all rock-forming minerals, a pAARM has been conducted on the samples used for coercivity analysis (see Trindade et al. (2001) for methodology). The results, plotted with AMS data for comparison on lower-hemisphere Schmidt projection for two of them (Fig. 5c), indicate similar fabrics for $pAARM_{5-20}$ and $pAARM_{20-80}$. Coaxiality between $pAARM_{5-20}$ and $pAARM_{20-80}$ controlled, respectively, by large and small magnetite grains, indicate a similar fabric for the different size of grain and exclude interactions between magnetite grains. In detail, for sample TJ58D2, coaxiality exists between AMS and $pAARM_{5-20}$ (representative of the shape-preferred orientation of coarse grains) while a deviation (in declination/inclination of about 16°) occurs for $pAARM_{20-80}$ (representative of the contribution of small magnetite grains) high and medium axes. For the second studied samples the strikingly coaxiality between AMS, $pAARM_{5-20}$ and $pAARM_{20-80}$ confirm the coaxiality of each magnetic contribution.

5.2. Intensity and shape of the magnetic fabric

The parameters P' and T, defined by Jelinek (1981) were calculated for the different AMS stations. These parameters are defined by the following expressions:

$$P' = \exp\sqrt{2\left[\left(\ln\frac{K_1}{K_m}\right)^2+\left(\ln\frac{K_1}{K_m}\right)^2+\left(\ln\frac{K_3}{K_m}\right)^2\right]}$$

and

$$T = \frac{2(\ln K_2 - \ln K_3)}{\ln K_1 - \ln K_3} - 1$$

P' describes the strength, or anisotropy degree, of the magnetic fabric. It varies from $P' = 1$ for an isotropic, spherical AMS ellipsoid to infinity. T is a shape parameter: the AMS ellipsoid varies from a prolate form for $-1 \leq T < 0$ (cigar-shaped for $T = -1$, i.e. $K_2 = K_3$), to an oblate form for $0 < T \leq 1$ (pancake-shaped for $T = 1$, i.e. $K_1 = K_2$) (Hrouda, 1982).

The value of P' ranges widely from 1.02 to 2.24 (Table 1 and Fig. 7), with an average (for all dikes) of 1.12, largely enhanced by the high values. Most P' values are in the range 1.02–1.1, which is similar to the values reported for basaltic dikes (Raposo and D'Agrella-Filho, 2000). The $P'-K_m$ plot (Fig. 7) shows that: (1) many data plot inside or close to the domain of the paramagnetic granitoids; the high $P'-K$ values correspond to rocks with high contents of sulfide and secondary oxides due to mechanical segregation on solid particles (Bagnold's effect); (2) for the TJ34 and TJ58 dikes, there is a strong correlation between the anisotropy degree and the magnetic susceptibility magnitude as commonly observed in ferromagnetic granites (Bouchez, 1997); and (3) for each dike, there is a strong correlation between sample position in the dike and the P' and K_m values, in agreement with the petrological and mineralogical (nature of the crystallized phases) observations.

Values of T range from -0.22 to 0.86 (Table 1), with an average value of $0.33 \pm$ RMS, indicating a planolinear to oblate AMS ellipsoid for the whole set of samples. The $T-P'$ plot (Fig. 7) illustrates the strong correlation between P' and T parameters and the asymmetrical disposition of the specimens on both sides of the $T = 0.5$ value. High P' values correspond to planolinear shape fabrics ($-0.5 < T < 0.5$) whereas low P' values correspond to oblate shape fabrics ($0.5 < T < 1$). In TJ58 and TJ56 symmetrical dikes (Fig. 7), the two margins have very similar magnetic anisotropy characteristics. As mentioned above, the high P' values are found preferentially at the wall of the larger dikes (Fig. 6a and b) if we consider TJ34 as a double dike. On the contrary, this situation is clearly inverted for the decimeter-size dikes (TJ56 and TJ58; Fig. 6c and d). The calculated values of T are not in agreement with the commonly supposed shape of the fabric ellipsoid along the rim, where a prolate ellipsoid is the best candidate for a simple shear. The same behavior has been observed for

rocks in which platy crystals represent the main magnetic phase. Platy crystals have not been observed in the Motru dikes. Nevertheless, our data could be compared with those of the 'normal magnetic fabric' of Callot et al. (2001), which is characterized by T values ranging from 0 to 1 (oblate domain) for very low values of P' (<1.05). Another way to explain this shape fabric is to consider the high values of theoretical strain recorded along the margins with the low values of the associated P', probably in relation to the interaction between markers for a high percentage of crystals (Arbaret et al., 1996) and debated below. These mechanic interactions can also play a major role concerning the T values.

5.3. Magnetic foliation and lineation

The axes of AMS ellipsoids have very regular orientations in the different dikes. Fig. 6a–d shows the projections of the dikes in the plane defined by the direction Z of the bodies (pole of the wall-dike) and horizontal direction (azimuth of the wall-dike). The stereographic projection of these corrected values have been plotted on Fig. 8.

The patterns of magnetic foliations K_1K_2 (perpendicular to K_3 magnetic direction) and lineations K_1 are roughly homogeneous. Two contrasting types of dike emplacement can be distinguished. (1) The thick dikes TJ34 and TJ30 are characterized by oblique sigmoidal foliation trajectories (Figs. 6a and b and 8A and B) indicative of a sinistral transcurrent structure in the way of Correa-Gomes et al. (2001). Local concave or convex morphologies near boundaries have been confirmed by field observations (penetrative cleavage along the walls). The lineations are not vertical everywhere (the plunge varies from 30° to 90°), which implies a horizontal component of the direction of the magmatic flow. Some of the low plunge values ($<50°$) are close to the dike boundaries of TJ30 and to a lesser extent to the eastern

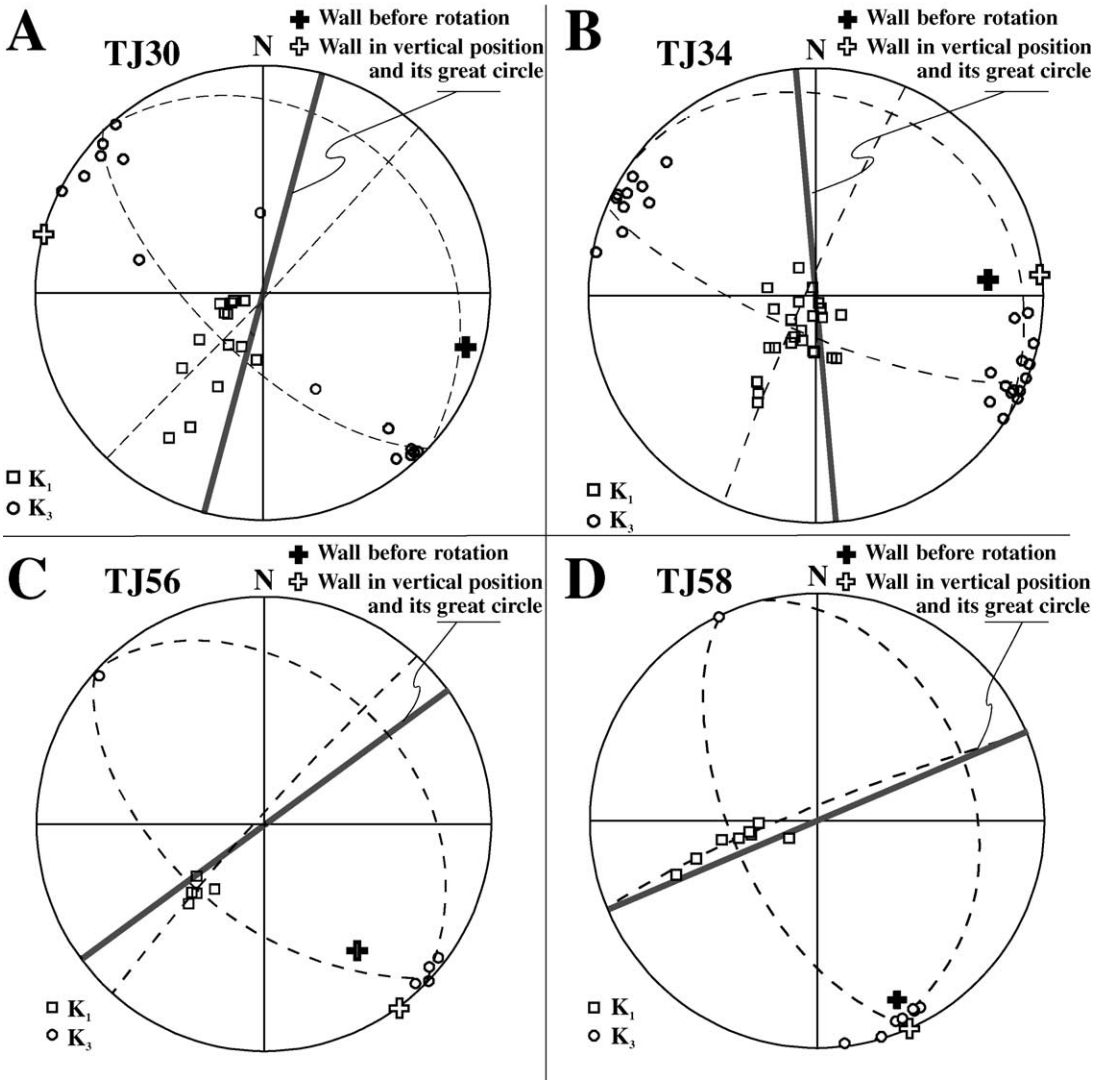

Fig. 8. Stereographic representation (Schmidt, lower hemisphere) for the four dikes with the wall tilted in a vertical position.

rim of TJ34 also. In the central part of the dikes, the values of plunge are less homogeneous (Fig. 6a and b) and probably correspond to variations of flowing regime and intensity of fabric between core and rim. (2) The thin TJ56 and TJ58 dikes have more homogeneous foliation and lineation patterns (Figs. 6c and d and 8C and D). TJ56 also shows an oblique foliation but no real sigmoidal pattern; TJ58 has slightly imbricate foliations between the two rim and foliations sub-parallel to the wall direction in the core (Figs. 6d and 8D) using the criteria of Moreira et al. (1999) and Callot et al. (2001). In agreement with the Callot et al. (2001) method, the AMS lineation (i.e. magmatic stretching direction) records a WSW–ENE flowing direction and not a real transcurrent movement.

6. Discussion

6.1. Deformation mechanism, magma rheology and fabric acquisition

The magnetic sub-fabric records the magmatic fabrics that are acquired during flowing, more particularly at the very late stage of emplacement, immediately before and after the local cooling. It is particularly important to discuss the rheological behavior of the magma immediately above the solidus to interpret the $P'-T$ parameters. The well-known fact that magma rheology changes drastically during the transition from hypersolidus to solidus conditions (e.g. Paterson et al., 1998) is used to understand the relationships between viscosity, temperature, percentage of crystals, and deformation mechanisms for basaltic magmas. The crystals percentage, melt polymerization and magma viscosity increase with decreasing temperature (Lofgren, 1980; Wickham, 1987; Cruden, 1990). As a consequence, the interactions between crystals and the magma–crystal relationship progressively change the behavior of the magma, from Newtonian ($<35\%$ crystals), to Binghamian and finally to power law behavior at high crystal content (e.g. Webb and Dingwell, 1990; Fernandez and Gasguet, 1994; Paterson et al., 1998). The mechanical behavior of crystals between the two margins of the dike (Bagnold, 1954; Komar, 1972a,b, 1976; Barrière, 1976) in a non-coaxial simple shear deformation integrates these parameters (Ildefonse and Fernandez, 1988; Ildefonse et al., 1992a,b; Nicolas, 1992).

Detailed microscopic observations on drilled samples show local crystal accumulation mainly of amphibole and biotite during the flow, possibly enhanced by late sulfide and oxide during retrogression and chilled margins that are often characterized by a deuteritic fine-grained matrix. Simple shearing along the wall induces mineral segregation inside the dike (Bagnold effect) and, consequently, rheological variations. The crystal-laden magma in the core zone of the dike can be considered as a Bingham mush, whereas the crystal-free marginal zones can be considered as a Newtonian liquid with a relatively high melt fraction. This rheological zoning of the dike involves a final fabric that can explain several features: (1) the maximum displacement occurs in the core zone of the dike, because the shearing is more important near the wall; (2) the observed correlation between the melt fraction and differential stress during emplacement (Wickham, 1987; see also Nicolas, 1992); and (3) the inverted correlation between the rate of deformation and the anisotropy of fabric ellipsoid (Arbaret et al., 1996, 2000, 2001).

The fabric is usually considered as being at a maximum at the margins of a dike. Nevertheless, the above points (2) and (3) constitute an apparent '*finite fabric paradox*'. Indeed, following point (2), the amount of crystal is at a maximum in the core and the differential stress too, while following point (3), for a high rate of deformation near the walls, anisotropy of fabric should be lower than in the core.

In fact, the fabric is not necessarily a good indicator of the rate of deformation recorded by the lithologies but is rather indicative of the rheological state of the magma during the late local cooling history. In that sense, a liquid with a low percentage of crystals affected by a strong shearing process does not necessarily record a stronger fabric than a crystal mush submitted to a lower deformation. The usual models of dike intrusions have to be discussed in relation to the intrusion of a heterogeneous magma (carrying variable amounts of suspended crystals); in that case, the central crystal mush can probably better record a slight increment of deformation. Moreover, the intensity of the observed final deformation state in terms of fabric is not representative of the γ increment of movement (Arbaret et al., 1996, 2000, 2001). As shown by these authors, a low intensity of the fabric is representative of a high γ value, whereas a high intensity can be related to a low shear strain in which there are only a few interacting particles. In the first case (high shear strain), the angle between the fabric and the shear plane is low, and there is a good correlation between the fabric lineation and the direction of flow. Thus, the anisotropy of magnetic susceptibility displays a good record of the final fabric but is not representative of γ. Hence, the P' parameter in symmetrical dikes has higher values in the central zone as well as in relation to a low γ value (here the surface and main direction of the fabric are very distinctive of a finite passive marker's strain ellipsoid model) according to the Arbaret relation, than with an evolution of the fabric across a cooling-related Binghamian dike where the flow continues in the core after cooling of the rim.

6.2. Significance of the magnetic parameters

The mapping of the magnetic parameters P', K_m and T, combined with the orientations of the axes $K_1-K_2-K_3$, inside the studied dikes has allowed two types of magnetic sub-fabric, symmetrical and asymmetrical, to be clearly

distinguished. This has important implications for the emplacement processes of the respective dikes.

For the thin symmetrical dikes (TJ56 and TJ58 in Fig. 9a), P' values are higher in the core of the body than along the rims. Petrographic observations have shown the classical crystal segregation (Platten, 1995) in the core zone and the aphyric texture (chilled margins) on the rims, illustrating the Bagnold effect (Bagnold, 1954; Barrière, 1976; Komar, 1972a,b, 1976). The variations in the magnitude of the anisotropy parameter P' are possibly related to (1) the variations of rheology during dike emplacement and/or (2) the lower shear strain recorded by the fabric (Arbaret et al., 1996, 2000, 2001). The accumulation of micro-phenocrysts (including the late sulfides and oxides) in the core of the dike explains the high values of the mean susceptibility and the Bingham behavior of the magma. This non-Newtonian zone has the ability to record more easily a short displacement registered as a relatively strong anisotropic fabric. The stronger deformation increment due to displacement near the wall rock in a non-coaxial deformation process is not easily recorded in magmas with Newtonian rheological behavior. Thus, the rims of the dikes do not present strong anisotropy in magnetic sub-fabric. The observed negative correlation between P' and T (Fig. 7) corresponds to a geometric evolution from an oblate shape fabric on the rim of the dike (high γ) to a plano-linear shape fabric in the core (lower γ).

The thick asymmetrical dikes (TJ34 and TJ30 in Fig. 9) present more peculiar features. The magnetic parameters and the bulk susceptibility are correlated with petrographic characteristics (as for symmetrical dikes), but the parameters inside the dike show asymmetrical distribution (Fig. 6) and, for TJ34, repetitive features, suggesting that it is, in fact, a composite dike or a dike-in-dike body. Magnetic foliations are oblique to wall dikes in the core and sub-parallel near the rim, displaying a sigmoidal foliation pattern. The parallelism of the magmatic surface near the rim is field observable in chilled margins by curvature of the erosion surfaces overprinting the foliation pattern. The lineations display apparent complex trajectories that

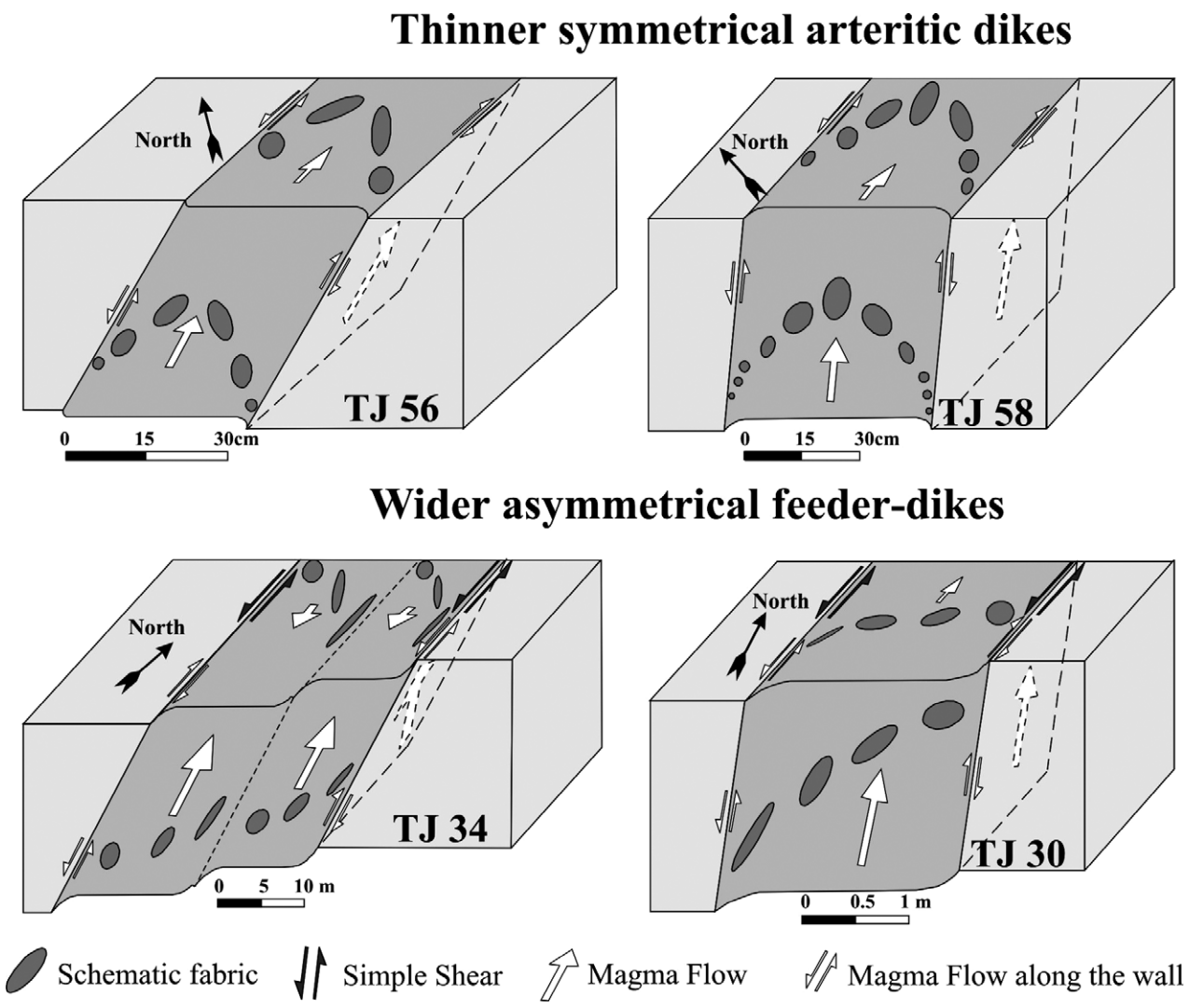

Fig. 9. Schematic sketches illustrating the relationship between magnetic sub-fabric, magmatic flowing and the dynamic of the wall rocks for each studied dike.

represent artifacts of the projection, because they have strong plunge (55° to 88°). Nevertheless, the horizontal component of the vector correlated with the sigmoidal surface trajectories has been used to estimate the sense of flowing and its participation in the bulk (magmatic-regional stress) fabric.

6.3. Symmetrical and asymmetrical dikes: a record of the regional Paleo-stress

The symmetrical or sub-symmetrical magnetic fabric of the thin dikes suggest that the regional stress field has only had a very weak effect on the dike laid in a particular orientation to the stress field (Correa-Gomes et al., 2001; Aubourg et al., 2002) and that the dike's fabric is mainly related to an internal differential stress due to a single magma pressure during the break-up propagation. According to theoretical investigations on dike injection (e.g. Delaney, 1987; Pollard, 1987; Turcotte et al., 1987), the emplacement of the thin dikes supposes a short-time injection and a rapid cooling, as observed on thin sections. The magnetic foliation K_1–K_2 is constant and sub-vertical between the two margins, as are those observed in several decimeter-thick dikes emplaced in cold country rocks (model b; Fig. 3). The oblique magnetic foliation observed in TJ58 could reflect a slight movement of the wall-dike, as suggested by Correa-Gomes et al. (2001). The thick (decameter-thick) TJ30 and TJ34 dikes and others that are comparable and still wider (up to 30 m) from the Motru area are strongly asymmetrical, which implies a horizontal displacement, presumably a sinistral transcurrent shearing regional strain field, overprinting the magmatic theoretical fabric. The sense of shearing indicates that the orientation of the mean stress vector σ_1 was close to the N–NW quadrant (N135° to N175°), not far from the mean direction of the thin dikes (Fig. 10). In this assumption, the lower stress vector σ_3 has to be close to the NE–E quadrant (N45° to N85°), near the direction of expansion of the thin symmetrical dike

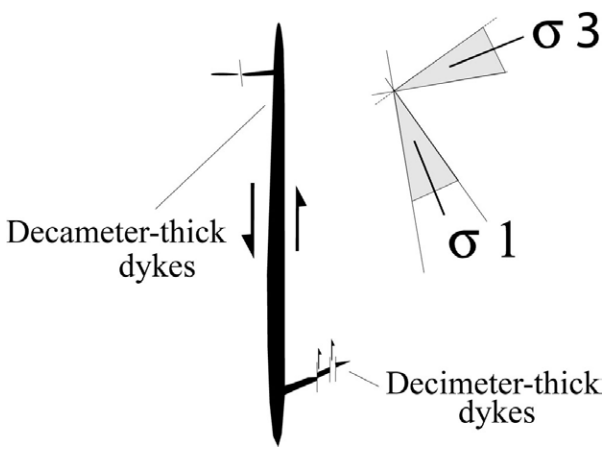

Fig. 10. Schematic sketch illustrating maps of the relation between the two dike populations (feeder and arteritic) and the interpretation of their dynamic emplacement.

population. Thin-dike emplacement could result from a traction process due to a relative differential amount of displacement along the thick dikes. Thus, the opening direction may be perpendicular to the mean direction of the dike, as observed in 'pull-apart' structures.

6.4. Implication to feeder volcanic processes

The two (symmetrical and asymmetrical) dike populations are characterized not only by their magnetic anisotropy but also by their petrographic texture, dike width and average orientation (Fig. 2A and B). Indeed, the thick (>1 m) dikes are asymmetrical; they correspond either to a single body or to a multiple dike-in-dike assemblage. They are characterized by a fine-grained texture and thin (centimeter-thick) chilled aphyric margins, and a significant proportion of pre-intrusion phases (essentially phenocrysts of tschermakite, plagioclase and sometimes biotite). The chilled margins commonly display late-magmatic shear structures parallel to the mean magnetic foliation. These dikes can be up to 1 km in length, depending on their width. They represent a quite large volume of sub-volcanic material in the area. The asymmetrical characters and the dike-in-dike emplacement suggest a relatively long magmatic activity, probably over large distances of flow.

By contrast, the thin (<1 m) symmetrical dikes frequently display an arteritic morphology with sharp ending and finger structures; they are limited in length, with no cartographic extension. Textures are commonly aphyric; chilled margins are present too, which implies a low crystal content during intrusion. They obviously represent a much smaller volume of material than the thick dikes. The symmetrical bodies do not record the regional stress field and involve rapid injection and cooling. Thus, we propose that the thick asymmetrical dikes can be considered as feeder dikes of the main volcanic activity in this area, whereas the contemporaneous, thin, symmetrical 'arteritic' dikes only record loss of magma in the country rocks. Our study on sub-volcanic dikes thus suggests that volcanic feeding by thick dikes is constrained by the regional stress field at a high level in the crust. In the same context, thin dikes cannot be considered as feeders but more probably correspond to local low extension injection in the anisotropy surface of the country rocks.

7. Conclusion

The Motru dike swarm (Southern Carpathians, Romania) is composed of two contemporaneous populations of intrusive bodies, thin (<1 m) and thick (several meters) dikes, each of them displaying specific petrological and structural features. This dike population has been interpreted in terms of emplacement mode and flow patterns. It has been shown that the fabrics of each dike type can be

related to a combination of flow pattern and wall displacement (Correa-Gomes et al., 2001). Our results show that the regional stress field has played a major role during the injection of the thick dikes. The record of this stress field in the dike fabrics implies a relatively long injection period and suggests that they can be considered as feeders of a high level volcanic activity. Moreover, this detailed AMS survey, focused on thin dikes, shows that investigation on dikes is a convenient way to understand the emplacement process as well as the regional stress field.

Acknowledgements

This work was partly supported by a grant from NATO for the field survey. We gratefully thank Prof. P. Launeau and an anonymous reviewer for their fruitful suggestions. Magnetic measurements (AMS) have been supported by CLDG La Rochelle (AMS). We thank also Lionel Esteban who has conducted Coercive and pAARM data at the Laboratory of Petrophysics of J.L. Bouchez (Paul-Sabatier University, Toulouse, France).

References

Arbaret, L., Diot, H., Bouchez, J.-L., 1996. Shape fabrics of particles in low concentration suspensions: 2D analogue experiments and application to tiling in magma. Journal of Structural Geology 18, 941–950.

Arbaret, L., Fernandez, A., Ježek, J., Ildefonse, B., Launeau, P., Diot, H., 2000. Analogue and numerical modeling of shape fabrics: application to strain and flow determination in magmas. Transactions of the Royal Society of Edinburgh—Earth Sciences 91, 97–109.

Arbaret, L., Mancktelow, N.S., Burg, J.P., 2001. Effect of shape and orientation on rigid particle rotation and matrix deformation in simple shear flow. Journal of Structural Geology 23, 113–125.

Archanjo, C.J., Trindade, R.I., Macedo, J.W.P., Araújo, M.G., 2000. Magnetic fabric of a basaltic dyke swarm associated with Mesozoic rifting in northeastern Brazil. Journal of South American Earth Sciences 13, 179–189.

Aubourg, C., Giordano, G., Mattei, M., Speranza, F., 2002. Magma flow in sub-aqueous rhyolitic dikes inferred from magnetic fabric analysis (Ponza Island, W. Italy). Physics and Chemistry of the Earth 27, 1263–1272.

Baer, G., 1995. Fracture propagation and magma flow in segmented dykes: field evidence and fabric analyses, Makhtesh Ramon, Israel. In: Baer, G., Heimann, M. (Eds.), Physics and Chemistry of Dykes, Balkema, Rotterdam, pp. 125–140.

Bagnold, R.A., 1954. Experiments on a gravity-free dispersion of large solid spheres in a newtonian fluid under shear. Proceedings of the Royal Society, London 225, 49–63.

Barrière, M., 1976. Flowage differentiation. Limitation of the "Bagnold effect" to the narrow intrusions. Contributions to Mineralogy and Petrology 55, 139–145.

Berza, T., 1978. Studiul mineralogic si petrografic al masivului granitoid de Tismana. An. Inst. Geol. Geofiz. LIII, 5–176.

Berza, T., Iancu, V., 1994. Variscan events in the basement of the Danubian nappes (South Carpathians). In: Berza T. (Ed.), Geological Evolution of the Alpine–Carpathian–Pannonian system, ALCAPA II, Field Guidebook. Rom. J. Tect. Reg. Geol. 75, pp. 93–104.

Berza, T., Seghedi, A., 1975. Complexul filonian presilurian din bazinul Motrului (Carpatii Meridionali). D.S. Inst. Geol. Geofiz. LXI/1, 131–149.

Berza, T., Seghedi, A., 1983. The crystalline basement of the Danubian units in the Central South Carpathians. An. Inst. Geol. Geofiz. LXI, 15–22.

Berza, T., Kräutner, H.G., Dimitrescu, R., 1983. Nappe structure of the Danubian window of the central South Carpathians. An. Inst. Geol. Geofiz. 60, 31–34.

Berza, T., Balintoni, I., Iancu, V., Seghedi, A., Hann, H.P., 1994. South Carpathians. In: Berza T. (Ed.), Geological Evolution of the Alpine–Carpathian–Pannonian system, ALCAPA II, Field Guidebook. Rom. J. Tect. Reg. Geol. 75, pp. 37–49.

Borradaile, G.J., Henry, B., 1997. Tectonic applications of magnetic susceptibility and its anisotropy. Earth-Science Reviews 42, 49–93.

Bouchez, J.L., 1997. Granite is never isotropic: an introduction to AMS studies of granitic rocks. In: Bouchez, J.L., Hutton, D.H.W., Stephen, W.E. (Eds.), Granite: From Segregation of Melt to Emplacement Fabrics, pp. 95–112. Kluwer Academic Publishers.

Callot, J.P., Geoffroy, L., Aubourg, C., Pozzi, J.P., Mege, D., 2001. Magma flow of shallow dykes from the East Greenland volcanic margin inferred from magnetic studies. Tectonophysics 335, 313–329.

Cañón-Tapia, E., 2001. Factors affecting the relative importance of shape and distribution anisotropy in rocks: theory and experiments. Tectonophysics 340, 117–131.

Cañón-Tapia, E., Walker, G.P.L., Herrero-Bervera, E., 1996. The internal structure of lava flows—insights from AMS measurements I: Near-vent a'a. Journal of Volcanology and Geothermal Research 70 (1-2), 21–36.

Correa-Gomes, L.C., Souza Filho, C.R., Martins, C.J.F.N., Oliveira, E.P., 2001. Development of symmetrical and asymmetrical fabrics in sheet-like igneous bodies: the role of magma flow and wall-rock displacements in theoretical and natural cases. Journal of Structural Geology 23, 1415–1428.

Coward, M.P., 1980. The analysis of flow profiles in a basaltic dyke using strained vesicles. Journal of the Geological Society, London 137, 605–615.

Cruden, A.R., 1990. Flow and fabric development during diapiric rise of magma. Journal of Geology 98, 681–698.

Delaney, P.T., 1987. Heat transfer during emplacement and cooling of mafic dykes. In: Halls, H.C., Fahrig, W.H. (Eds.), Mafic Dyke Swarms. Geological Society of Canada, Special Paper 34, pp. 31–46.

Duchesne, J.-C., Berza, T., Liégeois, J.P., Vander Auwera, J., 1998. Shoshonitic liquid line of descent from diorite to granite: the late Precambrian post-collisional Tismana pluton (South Carpathians, Romania). Lithos 45, 281–303.

Fernandez, A., Laporte, D., 1991. Significance of low symmetry fabrics in magmatic rocks. Journal of Structural Geology 13, 337–347.

Fernandez, A.G., Gasguet, D.R., 1994. Relative rheological evolution of chemically contrasted coeval magmas: example of the Tichka plutonic complex (Morocco). Contributions to Mineralogy and Petrology 116, 316–326.

Gay, N.C., 1968. The motion of rigid particles embedded in a viscous fluid during pure shear deformation of the fluid. Tectonophysics 5, 81–88.

Geoffroy, L., Callot, J.P., Aubourg, C., Moreira, M., 2002. Magnetic and plagioclase linear fabric discrepancy in dykes: a new way to define the flow vector using magnetic foliation. Terra Nova 14, 183–190.

Grégoire, V., Darrozes, J., Gaillot, P., Nédélec, A., Launeau, P., 1998. Magnetite grain shape fabric and distribution anisotropy vs. rock magnetic fabric: a three-dimensional case study. Journal of Structural Geology 20, 937–944.

Hargraves, R.B., Johnson, D., Chan, C.Y., 1991. Distribution anisotropy: the cause of AMS in igneous rocks? Geophysical Research Letters 18, 2193–2196.

Herrero-Bervera, E., Walker, G.P.L., Cañón-Tapia, E., Garcia, M.O., 2001. Magmatic fabric and inferred flow direction of dikes, conesheets and sill swarms, Isle of Skye, Scotland. Journal of Volcanology and Geothermal Research 106, 195–210.

Hrouda, F., 1982. Magnetic anisotropy of rocks and its application in geology and geophysics. Geophysical Surveys 5, 37–82.

Ildefonse, B., Fernandez, A., 1988. Influence of the concentration of rigid markers in a viscous medium on the production of preferred orientations. An experimental contribution, 1. Non-coaxial strain. In: Geological Kinematics and Dynamics (in honor of the 70th birthday of Hans Ramberg). Bulletin of the Geological Institute University Uppsala 14, pp. 55–60.

Ildefonse, B., Launeau, P., Bouchez, J.-L., Fernandez, A., 1992a. Effect of mechanical interactions on the development of shape preferred orientations: a two-dimensional experimental approach. Journal of Structural Geology 14, 73–83.

Ildefonse, B., Sokoutis, D., Mancktelow, N.S., 1992b. Mechanical interactions between rigid particles in a deforming ductile matrix. Analogue experiments in simple shear flow. Journal of Structural Geology 10, 1253–1266.

Jackson, M., Gruber, W., Marvin, J., Banerjee, S.K., 1988. Partial anhysteretic remanence and its anisotropy: applications and grainsize-dependence. Geophysical Research Letters 15, 440–443.

Jelinek, V., 1981. Characterization of the magnetic fabric of the rocks. Tectonophysics 79, 63–67.

Ježek, J., Schulmann, K., Segeth, K., 1996. Fabric evolution of rigid inclusions during coaxial and simple shear flows. Tectonophysics 257, 203–221.

Knight, D., Walker, M., 1988. Magma flow direction in dykes of Koolau Complex, Oahu, determined from magnetic fabric studies. Journal of Geophysical Research B5, 4301–4319.

Komar, P.D., 1972a. Mechanical interactions of phenocrysts and flow differentiation of igneous dikes and sills. Geological Society of America Bulletin 83, 973–988.

Komar, P.D., 1972b. Flow differentiation in igneous dikes and sills; profiles of velocity and phenocryst concentration. Geological Society of America Bulletin 83 (11), 3443–3447.

Komar, P.D., 1976. Phenocryst interactions and the velocity profile of magma flowing through dikes or sills. Geological Society of America Bulletin 87 (9), 1336–1342.

Kräutner, H.G., Nastaseanu, S., Berza, T., Stănoiu, I., Iancu, V., 1981. Metamorphosed Paleozoic in the South Carpathians and its relation to the pre-Paleozoic basement. Guide to Excursion A. Carpath. Balkan. Assoc. Congr. XII, Bucaresti, 116pp.

Kräutner, H., Berza, T., Dimitrescu, R., 1988. South Carpathians. In: Zoubek, V., (Ed.), Precambrian in Younger Fold Belts, Wiley, London, pp. 633–664.

Liégeois, J.P., Berza, T., Tatu, M., Duchesne, J.C., 1997. The neoproterozoic Pan-African basement from the Alpine Lower Danubian nappe system (South Carpathians, Romania). Precambrian Research 80, 281–301.

Lofgren, G., 1980. Experimental studies of the dynamic crystallization of silicate melts. In: Hargraves, R.B. (Ed.), Physics of Magmatic Processes. Princeton University Press, 585pp.

Manolescu, G., 1937. Etude géologique et pétrographique dans les Muntii Vulcan (Carpates Méridionales, Roumanie). An. Inst. Géol. Roum. XVIII, 79–172.

Marques, F.O., Coelho, S., 2003. 2-D shape preferred orientations of rigid particles in transtensional viscous flow. Journal of Structural Geology 25, 841–854.

Merle, O., 1998. Internal strain within lava flows from analogue modelling. Journal of Volcanology and Geothermal Research 81, 189–206.

Moreira, M., Geoffroy, L., Pozzi, J.-P., 1999. Magmatic flow in Azores hot spot dykes: preliminary results with anisotropy of magnetic susceptibility (AMS) in San Jorge Island. Comptes Rendus de l'Académie des Sciences - Series IIA - Earth and Planetary Science, 329, 15–22.

Nicolas, A., 1992. Kinematics in magmatic rocks with special reference to gabbros. Journal of Petrology 33, 891–915.

Paterson, S.R., Fowler, T.K. Jr, Schmidt, K.L., Yoshinobu, A.S., Yuan, E.S., Miller, R.B., 1998. Interpreting magmatic fabric patterns in plutons. Lithos 44, 53–82.

Pavelescu, L., 1953. Studiul geologic si petrographic al regiunii centrale si de Sud-Est a Muntilor Retezatului. An. Com. Geol. XXV, 119.

Platten, I.M., 1995. The significance of phenocryst distributions in chilled margins of dykes and sills for the interpretation of tip processes. In: Baer, G., Heimann, A. (Eds.), Physics and Chemistry of Dykes, Balkema, Rotterdam, pp. 141–150.

Pollard, D.D., 1987. Elementary fracture mechanics applied to the structural interpretation of dykes. In: Halls, H.C., Fahig, W.F. (Eds.), Mafic Dyke Swarms. Geological Association of Canada, Special Paper 34, pp. 5–24.

Raposo, M.I.B., D'Agrella-Filho, M.S., 2000. Magnetic fabrics of dyke swarms from SE Bahia State, Brazil: their significance and implications for Mesoproterozoic basic magmatism in the São Francisco Craton. Precambrian Research 99, 309–325.

Rochette, P., 1987. Magnetic susceptibility of the rock matrix related to magnetic fabric studies. Journal of Structural Geology 9, 1015–1020.

Rochette, P., Jackson, M., Aubourg, C., 1992. Rock magnetism and the interpretation of ansisotropy of magnetic susceptibility. Review of Geophysics 30, 209–226.

Rochette, P., Aubourg, C., Perrin, M., 1999. Is this magnetic fabric normal? A review and case studies in volcanic formation. Tectonophysics 307, 219–234.

Rust, A.C., Manga, M., 2002. Bubble shapes and orientations in low Re simple shear flow. Journal of Colloid and Interface Science 249, 476–480.

Savu, H., 1970. Structura plutonului granitoid de Susita si relatiile sale cu formatiunile autochtonului danubian (Carpatii Meridionali). D.S. Inst. Geol. LVI/5, 123–153.

Stănoiu, I., 1973. Zona Mehedinti–Retezat: o unitate paleogeografica si tectonica distincta a Carpatilor Meridionali. D.S. Inst. Geol. LIX/5, 127.

Tauxe, L., Gee, J.S., Staudigel, H., 1998. Flow direction from anisotropy of magnetic susceptibility data: the bootstrap way. Journal of Geophysical Research 103 (B8), 17775–17790.

Trindade, R.I.F., Bouchez, J.L., Bolle, O., Nédélec, A., Peschler, A., Poitrasson, F., 2001. Secondary fabrics revealed by remanence anisotropy: methodological analysis and examples from plutonic rocks. Geophysical Journal International 147, 310–318.

Turcotte, D.L., Emerman, S.H., Spence, D.A., 1987. Mechanics of dyke injection. In: Halls, H.C., Fahrig, W.H. (Eds.), Mafic Dyke Swarms. Geological Society of Canada, Special Paper 34, pp. 20–25.

Wada, Y., 1992. Magma flow directions inferred from preferred orientations of phenocrysts in a composite feeder dike, Mikaye-Jima. Japanese Journal of Volcanology and Geothermal Research 49, 119–126.

Webb, S.L., Dingwell, D.B., 1990. Non-Newtonian rheology of igneous melts at high stresses and strain rates: experimental results for rhyolite, andesite, basalt, and nephelinite. Journal of Geophysical Research 95, 15695–15701.

Wickham, S.M., 1987. The segregation and emplacement of granitic magmas. Journal of the Geological Society, London 144, 281–297.